

Crystal engineering of 6-carboxy-4-aryl-2,2'-bipyridine complexes: potent chelators with intrinsic intermolecular affinity

Hannah L. Dalton, Chris S Hawes, and Thorfinnur Gunnlaugsson

Cryst. Growth Des., **Just Accepted Manuscript** • Publication Date (Web): 16 Jun 2017

Downloaded from <http://pubs.acs.org> on June 16, 2017

Just Accepted

“Just Accepted” manuscripts have been peer-reviewed and accepted for publication. They are posted online prior to technical editing, formatting for publication and author proofing. The American Chemical Society provides “Just Accepted” as a free service to the research community to expedite the dissemination of scientific material as soon as possible after acceptance. “Just Accepted” manuscripts appear in full in PDF format accompanied by an HTML abstract. “Just Accepted” manuscripts have been fully peer reviewed, but should not be considered the official version of record. They are accessible to all readers and citable by the Digital Object Identifier (DOI®). “Just Accepted” is an optional service offered to authors. Therefore, the “Just Accepted” Web site may not include all articles that will be published in the journal. After a manuscript is technically edited and formatted, it will be removed from the “Just Accepted” Web site and published as an ASAP article. Note that technical editing may introduce minor changes to the manuscript text and/or graphics which could affect content, and all legal disclaimers and ethical guidelines that apply to the journal pertain. ACS cannot be held responsible for errors or consequences arising from the use of information contained in these “Just Accepted” manuscripts.

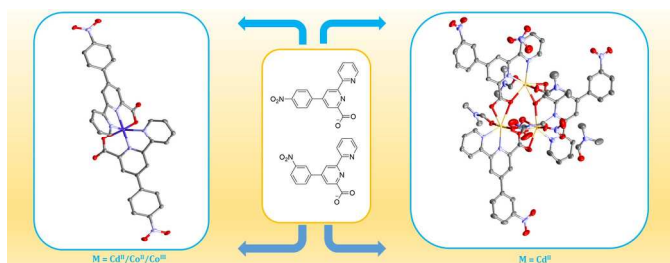


Crystal engineering of 6-carboxy-4-aryl-2,2'-bipyridine complexes: potent chelators with intrinsic intermolecular affinity

Hannah L. Dalton, Chris S. Hawes and Thorfinnur Gunnlaugsson*

School of Chemistry & Trinity Biomedical Sciences Institute, Trinity College Dublin, The University of Dublin, Dublin 2, Ireland.
Email: gunnlaut@tcd.ie

Herein we report the coordination chemistry and structural properties of two multifunctional terdentate 2,2'-bipyridine derivatives 4- and 3-(4-nitrophenyl)-2,2'-bipyridine-6-carboxylate, **L1/L2** respectively. We report 8 new coordination complexes with Cd^{II}, Co^{II} and Co^{III}, and study their behaviour in the crystalline phase with the view of establishing **L1** and **L2** as robust and functional chelators for use in extended metallosupramolecular systems. The divalent complexes [Cd(**L1**)₂]·H₂O **1**, [Cd(**L2**)₂] **2**, [Co(**L1**)₂] **5** and [Co(**L2**)₂] **7** are mononuclear complexes with distorted octahedral coordination geometries dictated by the two meridionally-coordinated **L1/L2** ligands. Also reported are two trivalent byproducts [Co(**L1**)₂]NO₃ **6** and [Co(**L2**)₂]NO₃ **8** which were formed in trace quantities during the initial screening of complexes **5** and **7**, respectively. The extended structures of these complexes are dominated by substantial intermolecular interactions, including anion···π hole interactions. Modification of the reaction conditions from **1** and **2** gives two closely-related trinuclear cluster species [Cd₃(**L1**)₃(NO₃)₂(DMF)₄]NO₃ **3** and [Cd₃(**L2**)₃(NO₃)₂(DMF)₄]NO₃·DMF **4**, in which three cadmium ions, with pentagonal bipyramidal coordination geometries, form disc-shaped assemblies with **L1/L2**, which undergo further weak interactions between neighbouring complexes in the crystalline state. With these outcomes **L1** and **L2** are established as exciting new building blocks for metallosupramolecular assemblies involving *d*-block metal ions.



Contact Author: Prof. Thorfinnur Gunnlaugsson
School of Chemistry and Trinity Biomedical Sciences Institute (TBSI)
Trinity College Dublin
Dublin 2, Ireland
Phone: +353-1-896 3459
Emails: gunnlaut@tcd.ie
<https://thorrigunnlaugsson.wordpress.com/>

1
2
3
4
5
6
7
8
9
10
11
12
13
14
15
16
17
18
19
20
21
22
23
24
25
26
27
28
29
30
31
32
33
34
35
36
37
38
39
40
41
42
43
44
45
46
47
48
49
50
51
52
53
54
55
56
57
58
59
60

Crystal engineering of 6-carboxy-4-aryl-2,2'- bipyridine complexes: potent chelators with intrinsic intermolecular affinity

*Hannah L. Dalton, Chris S. Hawes and Thorfinnur Gunnlaugsson**

School of Chemistry and Trinity Biomedical Sciences Institute, Trinity College Dublin, The

University of Dublin, Dublin 2, Ireland. Email: gunnlaut@tcd.ie

Abstract

Herein we report the coordination chemistry and structural properties of two multifunctional terdentate 2,2'-bipyridine derivatives 4- and 3-(4-nitrophenyl)-2,2'-bipyridine-6-carboxylate, **L1/L2** respectively. We report 8 new coordination complexes with Cd^{II}, Co^{II} and Co^{III}, and study their behaviour in the crystalline phase with the view of establishing **L1** and **L2** as robust and functional chelators for use in extended metallosupramolecular systems. The divalent complexes [Cd(**L1**)₂]·H₂O **1**, [Cd(**L2**)₂] **2**, [Co(**L1**)₂] **5** and [Co(**L2**)₂] **7** are mononuclear complexes with distorted octahedral coordination geometries dictated by the two meridionally-coordinated **L1/L2** ligands. Also reported are two trivalent byproducts [Co(**L1**)₂]NO₃ **6** and [Co(**L2**)₂]NO₃ **8** which were formed in trace quantities during the initial screening of complexes **5** and **7**, respectively. The extended structures of these complexes are dominated by substantial intermolecular interactions, including anion···π hole interactions. Modification of the reaction conditions from **1** and **2** gives two closely-related trinuclear cluster species [Cd₃(**L1**)₃(NO₃)₂(DMF)₄]NO₃ **3** and [Cd₃(**L2**)₃(NO₃)₂(DMF)₄]NO₃·DMF **4**, in which three cadmium ions, with pentagonal bipyramidal coordination geometries form disc-shaped assemblies with **L1/L2**, which undergo further weak interactions between neighbouring complexes in the crystalline state. With these outcomes **L1** and **L2** are established as exciting new building blocks for metallosupramolecular assemblies involving *d*-block metal ions.

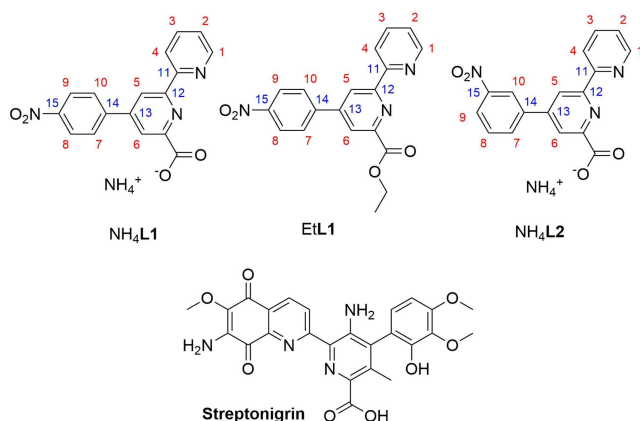
Introduction

In the on-going drive towards new functional supramolecular systems, a constant need exists for the discovery and development of new ligand systems, binding motifs and molecular scaffolds, in order to diversify the existing chemical toolbox and rationally pursue specific applications.¹⁻³ To this end, significant progress has been made recently in establishing modular ligand sets for further development into supramolecular systems.^{4,5} Doing so requires a thorough basis in the fundamental coordination chemistry and structural trends of archetypal systems, to establish the necessary understanding of the subtle geometric and electronic effects which are well known to strongly influence the bulk properties of such systems.⁶⁻⁹ The polypyridine family of ligands are well-known metallocupramolecular ligand scaffolds, widely exploited in transition metal coordination chemistry, due to the predictable coordination behaviour and favourable electronic and magnetic properties of bipyridine and terpyridine *d*-metal ion complexes.^{10,11} These structures have found myriad applications, including as dye-sensitized solar cells,¹² redox photocatalysts,¹³ molecular electronics and spin crossover devices.¹⁴⁻¹⁶ As well-established starting points, functional 2,2'-bipyridine derivatives are ideally suited for the installation of new substitution patterns and functional groups.¹⁷ Although direct derivatisation of the deactivated pyridine ring itself can be synthetically cumbersome compared to other nitrogen heterocycles,¹⁸ new synthetic methods are continually emerging for the synthesis of functional bipyridine ligands.¹⁹⁻²⁰

The scope of possible modification to the 2,2'-bipyridine backbone includes the incorporation of additional chelating groups at the 6 and/or 6' positions, with the view of increasing the metal binding affinity, while functionalisation at the 4 and/or 4' positions allows for the grafting of additional chemical functionality, or structural handles, for engineering intermolecular

1
2
3 interactions.²¹⁻²³ Work by Kruger *et al.* has demonstrated the utility of a carboxylate moiety in
4 the 6 position for the generation of polymeric assemblies involving strong chelation of the
5
6
7
8 tridentate *N,N,O*-binding pocket to Cu^{II} ions with bridging through additional carboxylate
9
10
11 functionality.²⁴ In that case, the unsymmetric substitution of the bipyridine skeleton was
12
13 achieved by partial decarboxylation of the tetracarboxylic acid precursor. Some examples are
14
15 known of simple bipyridine ligands unsymmetrically substituted with a carboxylate group at a
16
17 single 6 position,^{25,26} although the corresponding 1,10-phenanthroline analogue is more
18
19 common.²⁷⁻³⁰

21
22 Examples of structurally characterised 6-carboxy-4-aryl-2,2'-bipyridine derivatives are
23
24 relatively uncommon, although the naturally occurring antitumor antibiotic Streptonigrin is one
25
26 such fascinating example, **Scheme 1**.^{31,32} Interestingly, the coordination of metal ions to
27
28 Streptonigrin has been shown to promote DNA binding and lead to an enhanced degree of
29
30 toxicity. However, to date, only three reports have emerged of metal complexes of 6-carboxy-4-
31
32 aryl-2,2'-bipyridine ligands, which can be considered simplified tridentate analogues of
33
34 Streptonigrin in metal binding affinity without the added complication of the redox-active
35
36 quinone ring.³³⁻³⁵ In most of these cases, lanthanide ions were employed in order to access the
37
38 photophysical antenna properties of the extended aromatic ligand backbone, and to provide a
39
40 better geometric match with the steric demands of the ligand being better suited to high
41
42 coordination numbers.³⁶ As such, the coordination chemistry of these systems with *d*-block metal
43
44 ions remains a fertile area for further exploration. Here we describe the coordination chemistry
45
46 of 4-(4/3-nitrophenyl)-2,2'-bipyridine-6-carboxylate (**L1/L2**, Scheme 1) with cobalt and
47
48 cadmium ions, elucidating two unique crystalline phases for each combination of metal and
49
50
51
52
53
54
55
56
57
58
59
60 ligand, and contrast the structural properties of the resulting 8 compounds.



Scheme 1 Structures of NH₄L1, EtL1 and NH₄L2, with numbering scheme for NMR assignment and Streptonigrin

Experimental

The chalcone precursors, **Scheme 2**, were synthesised according to literature procedures.^{37,38} All other reagents and solvents were purchased from Sigma-Aldrich, Merck or Fisher Scientific, were of reagent grade or better, and were used as received. All NMR spectra were recorded using either a 400 MHz Bruker Avance III or 600 MHz Bruker Avance II spectrometer, operating at 400.1 or 600.1 MHz for ¹H NMR and 100.2 or 150.2 MHz for ¹³C NMR. Chemical shifts are reported in ppm referenced relative to the internal residual solvent signals. Electrospray mass spectra were recorded on a Micromass LCT spectrometer or a MALDI QToF Premier, running Mass Lynx NT V 3.4 on a Waters 600 controller connected to a 996 photodiode array detector with HPLC-grade methanol or acetonitrile. High resolution mass spectra were determined by a peak matching method, using leucine enkephaline (Tyr-Gly-Gly-Phe-Leu) as the standard

1
2
3 reference ($m/z = 556.2771$). All accurate masses were reported within ± 5 ppm. Melting points
4
5 were determined using an IA9000 digital melting point apparatus in air and are uncorrected.
6
7
8 Infrared spectra were recorded on a Perkin Elmer Spectrum One FT-IR spectrometer fitted with a
9
10 Universal ATR Sampling Accessory. Elemental analyses were carried out at the Microanalytical
11
12 Laboratory, School of Chemistry and Chemical Biology, University College Dublin.
13
14 Thermogravimetric analysis was performed using a Perkin-Elmer Pyris 1 TGA instrument, with
15
16 samples (1 – 5 mg) mounted in alumina pans and heated in the range 25 – 500 °C at a rate of 5
17
18 °C/min under a constant N₂ flow of 20 mL/min. X-ray powder diffraction patterns were
19
20 measured on a Bruker D2 Phaser instrument operating using Cu K α ($\lambda = 1.54178$ Å) radiation
21
22 and a Lynxeye detector at room temperature, with samples mounted on a zero-background
23
24 silicon single crystal sample stage. The patterns collected at room temperature were compared
25
26 with the patterns simulated from the single crystal data (collected at 100K) to establish phase
27
28 purity of each crystalline material (Supporting Information).
29
30
31
32
33
34
35

36
37 *Synthesis of 4/3-(nitrophenyl)-2,2' bipyridine-6-carboxylate (L1 and L2, respectively)*

38
39 The appropriate chalcone (2.05 g, 1 eq, 9.04 mmol), 2-pyridacyl pyridinium iodide (1.79 g, 1
40
41 eq, 9.04 mmol) and ammonium acetate (5.74 g, 8 eq, 72.39 mmol) were added to H₂O (80 mL)
42
43 and heated under reflux for 5 hrs. The resulting precipitate was isolated by filtration and washed
44
45 with H₂O (2 × 50 mL) and acetone (2 × 50 mL) and air-dried, to yield **L1/L2** as off-white flaky
46
47 solids. In both cases, the solids obtained analysed for ammonium salts or mixed phases of the
48
49 type [(HL)_x(NH₄L)_{1-x}]; **L1** was obtained as the ammonium salt hemipentahydrate
50
51 NH₄**L1**·2.5H₂O (x = 0), while **L2** exhibited the bulk formula [(HL**2**)_{0.2}(NH₄L**2**)_{0.8}]·2.33H₂O.
52
53
54 Both materials were characterised and reacted onwards using these formulae.
55
56
57
58
59
60

1
2
3
4
5
6 **L1:** Yield 1.83g (53%). m.p. 238-240 °C (decomp.); Found C, 53.54; H, 4.51; N, 14.37;
7
8 Calculated for $C_{17}H_{11}N_3O_4 \cdot 2.5H_2O$ [$NH_4L1 \cdot 2.5H_2O$] C, 53.26; H, 4.99; N, 14.62%; m/z (HR-
9
10 ESI⁻) 320.0671 ($[M-H]^-$, calculated for $C_{17}H_{10}N_3O_4$ 320.0667); δ_H (DMSO- d_6 , 400 MHz) 8.66
11
12 (H_5 , d, $J = 1.8$ Hz, 1H), 8.51 (H_4 , d, $J = 8.0$ Hz, 1H), 8.38 (H_{9+8} , d, $J = 8.9$ Hz, 2H), 8.24 (H_6 , d, J
13
14 = 1.8 Hz, 1H), 8.16 (H_{10+7} , d, $J = 8.8$ Hz, 2H), 8.00 (H_3 , td, $J = 7.7$, 1.8 Hz, 1H), 7.50 (H_2 , ddd, J
15
16 = 7.4, 4.7, 1.0 Hz, 1H); δ_C (DMSO- d_6) 167.6 (COO), 157.6 (C_{16}) 155.2 (C_{11}), 155.1 (C_{12}) 149.2
17
18 (C_1), 147.7 (C_{15} -NO₂), 145.9 (C_{13}), 144.2 (C_{14}), 137.4 (C_3), 128.3 (C_{8+7}), 124.7(C_2), 124.3
19
20 (C_{9+10}), 121.3 (C_6), 121.1 (C_4), 117.8 (C_5); ν_{max} (ATR, cm^{-1}) 2981, 1588, 1510, 1415, 1330,
21
22 1256, 1104, 1003, 855, 788, 764, 752.
23
24
25
26
27
28

29 **L2:** Yield 1.62 g (48%). m.p. 219-221 °C (decomp.); Found C, 54.37; H, 4.17; N, 14.36;
30
31 Calculated for $[(HL2)_{0.2}(NH_4L2)_{0.8}] \cdot 2.33H_2O$ C, 54.17; H, 4.83; N, 14.12%; m/z (HR-ESI⁺)
32
33 322.0828 ($[M+H]^+$, calc. for $C_{17}H_{12}N_3O_4$ 322.0832); δ_H (600 MHz, DMSO- d_6) 8.70 (H_1 , d, $J =$
34
35 4.0 Hz, 1H), 8.64 (H_5 , d, $J = 1.7$ Hz, 1H), 8.56 (H_{10} , t, $J = 1.8$ Hz, 1H), 8.49 (H_4 , d, $J = 7.9$ Hz,
36
37 1H), 8.32 (H_{7+8} , dd, $J = 8.0$, 2.0 Hz, 2H), 8.23 (H_6 , d, $J = 1.8$ Hz, 1H), 7.97 (H_3 , td, $J = 7.8$, 1.7
38
39 Hz, 1H), 7.82 (H_9 , t, $J = 8.0$ Hz, 1H), 7.46 (H_2 , ddd, $J = 7.4$, 4.8, 1.0 Hz, 1H); δ_C (DMSO- d_6 , 600
40
41 MHz) 168.3 (COO), 158.8 (C_{16}), 155.8 (C_{12}), 155.7 (C_{11}), 149.6 (C_1), 149.0 (C_{18} - NO₂), 146.5
42
43 (C_{13}), 139.9 (C_{14}) 137.9 (C_3), 133.9 (C_7), 131.4 (C_9) 124.7 (C_2), 124.2 (C_8), 121.9 (C_{10}), 121.6
44
45 (C_4), 121.6 (C_6), 118.0 (C_5); ν_{max} (cm^{-1}) 2981,1579, 1516, 1413, 1316, 1105, 1001, 885, 854,
46
47 788,751, 685.
48
49
50
51
52
53
54

55 **Synthesis of Ethyl-4-(nitrophenyl)-2,2'-bipyridine-6-carboxylate (EtL1)**

56
57
58
59
60

L1 (1.0 g, 1 eq, 2.6 mmol) was suspended in EtOH (80 mL) and SOCl₂ (0.7 mL, 3.7 eq, 9.6 mmol) and heated to 80 °C for 24 hrs. The solvent was removed by vacuum distillation, and the resulting hydrochloride salt was taken up in H₂O (50 mL) and neutralised with sodium bicarbonate solution (3 x 15 mL). The precipitated **EtL1** was obtained by filtration as a beige solid (0.97 g, quant.). m.p 182-184 °C (decomp.); Found C, 62.16; H, 4.09; N, 11.21; Calculated for C₁₉H₁₅N₃O₄·H₂O C, 62.12; H, 4.66; N, 11.44%; *m/z* (HR-ESI⁺) 350.1156 ([M+H]⁺ calc. for C₁₉H₁₆N₃O₄ 350.1141); δ_H (400 MHz, DMSO) 8.91 (H₅, s, 1H), 8.77 (H₁, d, *J* = 4.2 Hz, 1H), 8.48 (H₄, d, *J* = 7.9 Hz, 1H), 8.43 (H₇₊₁₀, d, *J* = 8.5 Hz, 2H), 8.40 (H₆, s, 1H), 8.22 (H₈₊₉, d, *J* = 8.6 Hz, 2H), 8.06 (H₃, t, *J* = 7.6 Hz, 1H), 7.56 (H₂, m, 1H), 4.47 (CH₂, q, *J* = 7.1 Hz, 2H), 1.42 (CH₃, t, *J* = 7.1 Hz, 3H). δ_C (DMSO-d₆) 164.4 (COO), 156.4 (C₁₂), 153.9 (C₁₁), 149.5 (C₁), 148.7 (C₁₅), 148.1 (C₁₅-NO₂) 147.5 (C₁₃), 142.8 (C₁₄), 137.7 (C₃) 128.7 (C₇₊₉) 125.0 (C₂) 124.4 (C₈₊₁₀) 122.6 (C₆) 121.2 (C₅) 121.0 (C₄), 61.6 (CH₂), 14.2 (CH₃); ν_{max} (cm⁻¹) 3116, 3088, 2983, 2937, 1752, 1584, 1513, 1426, 1350, 1235, 1167, 1081, 1024, 904, 850, 783, 752, 695, 620.

Synthesis of [Cd(L1)₂]·H₂O **1**

Cadmium nitrate tetrahydrate (8 mg, 26 μmol) was dissolved in DMF:H₂O (2:1, 3 mL) and **EtL1** (10 mg, 27 μmol) was added. The reaction mixture was sealed in a Teflon-capped vial and heated at 80 °C for 8 hrs. The resulting colourless crystals were isolated by filtration to give **1**. Yield 7 mg, 35 %. m.p (decomp.) >280 °C; Found: C, 52.49; H, 2.72; N, 10.7%; calculated for C₃₄H₂₂CdN₆O₉ C, 52.97%; H, 2.87; N, 10.9%; ν_{max} (ATR, cm⁻¹) 3398, 3072, 1632, 1599, 1556, 1513, 1482, 1430, 1375, 1344, 1312, 1246, 1164, 105, 1009, 891, 860, 824, 796, 756, 719, 683, 664, 637, 600, 554. Phase purity was established by X-ray powder diffraction (Supporting Information)

Synthesis of [Cd(L2)₂] 2

Cadmium nitrate tetrahydrate (8 mg, 26 μmol) was dissolved in DMF:H₂O (2:1, 3 mL) and L2 (10 mg, 26 μmol) was added. The reaction mixture was sealed in a Teflon-capped vial and heated at 100 °C for 14 hrs. The resulting colourless crystals were isolated by filtration to give 2 which, as discussed in the text, unavoidably contained a trace quantity of inorganic impurities. Yield 3mg, 15%. m.p (decomp.) >280 °C; Found C, 53.33; H, 2.57 N, 10.95% calculated for C₃₄H₂₀CdN₆O₈ C, 54.23; H, 2.67; N, 11.16%; ν_{max} (ATR, cm⁻¹) 3059, 1635, 1602, 1577, 1522, 1485, 1422, 1415, 1644, 1305, 1282, 1245, 1164, 1078, 1020, 879, 797, 762, 750, 741, 723, 695, 667, 631, 597, 569. Phase purity was established by X-ray powder diffraction (Supporting Information)

Synthesis of polynuclear complexes [Cd₃(L1)₃(NO₃)₂(DMF)₄]NO₃ 3 and [Cd₃(L2)₃(NO₃)₂(DMF)₄]NO₃·DMF 4

Cadmium nitrate tetrahydrate (18 mg, 58 μmol) was dissolved in DMF (0.5 mL) and EtL1/L2 (20 mg, 54/52 μmol) was added. The reaction mixture was sealed in a Teflon-capped glass vial and heated at 100 °C for 18 hrs. On cooling to room temperature, the resulting colourless crystals were isolated by filtration. The solvent content was found to be variable depending on the age and drying conditions of the isolated sample, as discussed in the text.

[Cd₃(L1)₃(NO₃)₂(DMF)₄]NO₃ 3: Yield 18 mg, 56 %. m.p (decomp.) >280 °C; Found C 40.57; H, 2.81; N, 11.33; calculated for C₅₁H₃₀N₁₂O₂₁Cd₃·3DMF·1.5H₂O C, 40.45; H, 2.84; N, 11.47%

1
2
3 ν_{\max} (ATR, cm^{-1}) 3389, 2935, 1641, 1585, 1555, 1516, 1447, 1410, 1383, 1342, 1299, 1248,
4
5 1107, 1075, 1035, 1009, 908, 857, 799, 776, 754, 688, 665, 633, 618, 598, 586, 576. Phase purity
6
7 was established by X-ray powder diffraction (Supporting Information)
8
9

10
11
12 [Cd₃(L2)₃(NO₃)₂(DMF)₄]NO₃·DMF **4**: Yield 12 mg, 38 %. m.p (decomp.) >280 °C; Found C
13 40.54; H, 2.65; N, 11.37; calculated for C₅₁H₃₀N₁₂O₂₁Cd₃·3DMF·1.5H₂O C, 40.45; H, 2.84; N,
14 11.47%; ν_{\max} (ATR, cm^{-1}) 3387, 3066, 1638, 1599, 1580, 1553, 1525, 1482, 1424, 1380, 1347,
15 1308, 1246, 1163, 1109, 1075, 1050, 1019, 888, 797, 781, 741, 719, 692, 670, 625, 557. Phase
16
17 purity was established by X-ray powder diffraction (Supporting Information)
18
19
20
21
22
23
24

25 26 27 **Synthesis of [Co(L1/L2)₂] **5** and **7****

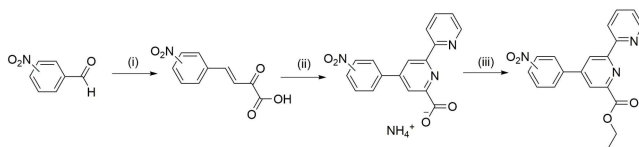
28
29 Cobalt(II) nitrate hexahydrate (3 mg, 10 μmol) was dissolved in DMF:H₂O (1:1, 3 mL) and
30
31 **EtL1/L2** (10 mg, 27/26 μmol) was added. The reaction mixture was sealed and heated at 100 °C
32
33 for 18 hrs. On cooling to room temperature, the resulting orange rod shaped crystalline material
34
35 was isolated by filtration.
36
37
38
39

40
41 [Co(L1)₂] **5**: Yield 3 mg, 43 %. m.p (decomp.) >280 °C; Found: C, 57.89; H, 2.76; N, 11.97;
42
43 calculated for C₃₄H₂₀CoN₆O₈ C, 58.37; H, 2.88; N, 12.01%; ν_{\max} (cm^{-1}) 3070, 2284, 2163, 1981,
44
45 1931, 1638, 1604, 1525, 1482, 1442, 1421, 1347, 1310, 1280, 1247, 1186, 1162, 1124, 1084,
46
47 1070, 1024, 972, 938, 898, 890, 823, 880, 793, 764, 754, 741, 730, 724, 694, 669, 628, 608, 577,
48
49 562 . Phase purity was established by X-ray powder diffraction (Supporting Information)
50
51
52
53
54
55
56
57
58
59
60

[Co(L2)₂] **7** Yield 6 mg, 86%. m.p (decomp.) > 280 °C; Found C, 57.86; H, 2.76; N, 11.72; calculated for C₃₄H₂₀CoN₆O₈ C, 58.37; H, 2.88, N, 12.01%; ν_{\max} (ATR, cm⁻¹) 3068, 1638, 1604, 1526, 1482, 1421, 1347, 1280, 1161, 1123, 1071, 1005, 898, 880, 823, 793, 764, 754, 741, 684, 628, 607, 559. Phase purity was established by X-ray powder diffraction (Supporting Information).

Synthesis of mixed Co^{II}/Co^{III} phases containing [Co(L1/L2)₂]NO₃ impurity **6** and **8**

Cobalt(II) nitrate hexahydrate (8 mg, 27 μ mol) was added to DMF (1 mL) and EtL1/L2 (10 mg, 27/26 μ mol) was added. The reaction mixture was sealed and heated at 100 °C for 24 hrs, giving a red crystalline solid which contained both Co^{II}/Co^{III} phases. Individual crystals of **6** and **8** were manually isolated from this mixture for single crystal X-ray diffraction analysis.



Scheme 2. Synthetic pathway for NH₄L1, EtL1 and NH₄L2 from benzaldehyde precursors; (i) sodium pyruvate, H₂O/EtOH, 2M NaOH/HCl (ii) Pyridacyl pyridinium iodide, ammonium acetate, H₂O^{37,38} (iii) SOCl₂, EtOH.

X-ray Crystallography

Structural and refinement parameters are presented in Table 1. All diffraction data were collected using a Bruker APEX-II Duo dual-source instrument using graphite-monochromated Mo K α ($\lambda = 0.71073$ Å) or microfocus Cu K α ($\lambda = 1.54178$ Å) radiation as specified. Datasets were collected using ω and ϕ scans with the samples immersed in oil and maintained at a constant temperature of 100 K using a Cobra cryostream. The data were reduced and processed

1
2
3 using the Bruker APEX suite of programs.³⁹ Multi-scan absorption corrections were applied
4
5 using SADABS.⁴⁰ The diffraction data were solved using SHELXT and refined by full-matrix
6
7 least squares procedures using SHELXL-2015 within the OLEX-2 GUI.⁴¹⁻⁴³ The functions
8
9 minimized were $\Sigma w(F_o^2 - F_c^2)$, with $w = [\sigma^2(F_o^2) + aP^2 + bP]^{-1}$, where $P = [\max(F_o)^2 + 2F_c^2]/3$. All non-
10
11 hydrogen atoms were refined with anisotropic displacement parameters. All hydrogen atoms
12
13 were placed in calculated positions and refined with a riding model, with isotropic displacement
14
15 parameters equal to either 1.2 or 1.5 times the isotropic equivalent of their carrier atoms. In cases
16
17 where U_{ij} or position restraints were necessary, these were employed sparingly and only for the
18
19 purpose of maintaining chemically sensible geometries and ADPs. Specific refinement strategies
20
21 are outlined in the combined crystallographic information file. CCDC 1544479-1544485.
22
23
24
25
26
27
28
29
30
31
32
33

34 **Results and Discussion**

35 36 37 38 **Ligand Synthesis**

39
40
41 The syntheses of **L1** and **L2** were based on modified literature procedures.³⁷⁻³⁸ The appropriate
42
43 nitrobenzaldehyde was reacted with sodium pyruvate to generate the precursor chalcone, which
44
45 was subjected to a Michael addition with 2-pyridacyl pyridinium iodide to yield the dipyrityls
46
47 **L1** and **L2**, respectively (Scheme 1). The bulk formulations of **L1** and **L2** in the solid form were
48
49 ascertained by elemental analysis as ammonium salts^{34,35} or mixtures of protonation states (see
50
51 experimental), and all solution-phase characterisation was consistent with the expected species in
52
53 solution. Largely due to the poor solubility of these compounds and the resulting complexes, the
54
55
56
57
58
59
60

1
2
3 short-wavelength absorption maxima of the electron-deficient aromatic chromophores ($\lambda_{\max} =$
4 280 nm or below, in both cases) and lack of any measurable fluorescence, no meaningful
5 information could be derived as to their solution phase coordination behaviour with divalent
6 cadmium or cobalt ions through UV-Visible absorption studies. As such, the discussion herein is
7 focused on the coordination chemistry of **L1** and **L2** in the crystalline phase.
8
9

10 While the formulation of **L2** obtained from the reaction mixture proved sufficiently soluble for
11 further reaction under solvothermal conditions, we encountered difficulties with the very low
12 solubility of $[\text{NH}_4\text{L1}]$ in common solvents, which hindered its reactivity with metal ions. Instead,
13 relying on the well-known tendency for ester groups to undergo metal-mediated *in situ*
14 hydrolysis at high temperatures,⁴⁴ the ethyl ester **EtL1** was instead employed as a feedstock for
15 these reactions. The ester was prepared using a thionyl chloride-mediated esterification of **L1**
16 and was used in all subsequent preparations, which provided an efficient route to the desired
17 complexes.
18
19
20
21
22
23
24
25
26
27
28
29
30
31
32
33
34
35

36 **Synthesis and structure of mononuclear Cd complexes of L1 and L2**

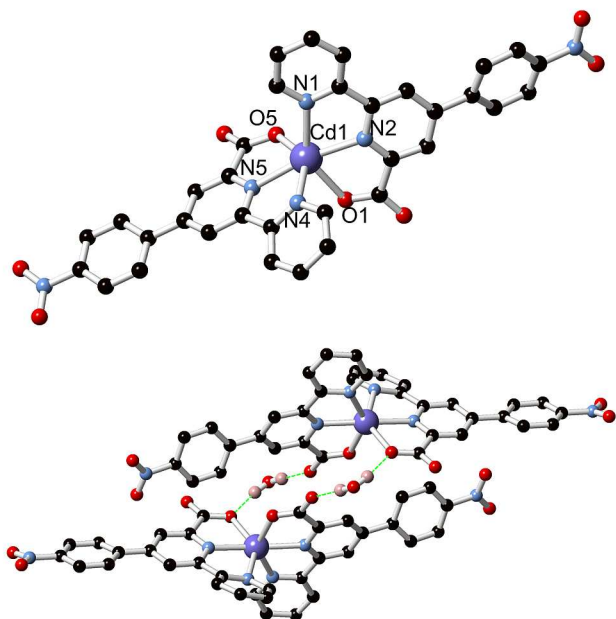
37
38
39
40

41 *Structure of $[\text{CdL1}_2]\cdot\text{H}_2\text{O}$ 1*

42

43 The reaction of **EtL1** in a 2:1 DMF:H₂O mixture with cadmium nitrate tetrahydrate at 100 °C
44 yielded pale yellow crystalline material after 18 hrs. The single crystal X-ray diffraction data for
45 $[\text{Cd}(\text{L1})_2]\cdot\text{H}_2\text{O}$ **1** were solved and refined in the triclinic space group *P*-1. The asymmetric unit
46 contains two **L1** molecules deprotonated and coordinating to a cadmium(II) ion, and a non-
47 coordinating water molecule (Figure 1). Two non-equivalent ligands coordinate to the cadmium
48 ion in a distorted octahedral geometry providing narrow *cis* bite angles of 71.27(7)° and
49
50
51
52
53
54
55
56
57
58
59
60

1
2
3 69.87(7)° for N2-Cd1-O1 and N5-Cd1-O5, respectively, and 69.46(7)° and 69.69(7)° for N2-
4
5 Cd1-N1 and N4-Cd1-N5, respectively. These angles give a large octahedral distortion parameter
6
7 Σ of 195°,⁴⁵ consistent with a size mismatch between the cadmium ion and the ligand binding
8
9 pocket when coordinating in a bis-tridentate mode. The Cd-N bonds to the outer pyridine
10
11 nitrogen atoms N1 and N4 (2.369(2) and 2.389(2) Å) are longer than the bonds to the central
12
13 pyridine nitrogen atoms N2 and N5 (2.283(2) and 2.285(2) Å) and the carboxylate oxygen atoms
14
15 O1 and O5 (2.306(2) and 2.329(2) Å, respectively). Both ligands exhibit some distortion from
16
17 complete planarity; the nitrophenyl rings are each inclined from their attached pyridine rings
18
19 with torsion angles 24.0(3)° (C13-C12-C8-C9) and 12.7(3)° (C34-C29-C25-C26). A very large
20
21 dihedral angle is also observed between two coordinating pyridine rings on one molecule of **L1**,
22
23 with the torsion angle (N5-C23-C22-N4) of 18.9(3) ° falling outside the 98th percentile of known
24
25 torsions for chelating 2, 2'-bipyridine groups (Supporting Information).
26
27
28
29
30
31



1
2
3 **Figure 1** Structure of complex **1**, with labelling scheme for coordinating atoms (top) and
4 showing hydrogen bonding interactions between adjacent complexes *via* lattice water molecules
5 (bottom). Selected hydrogen atoms are omitted for clarity.
6
7
8
9

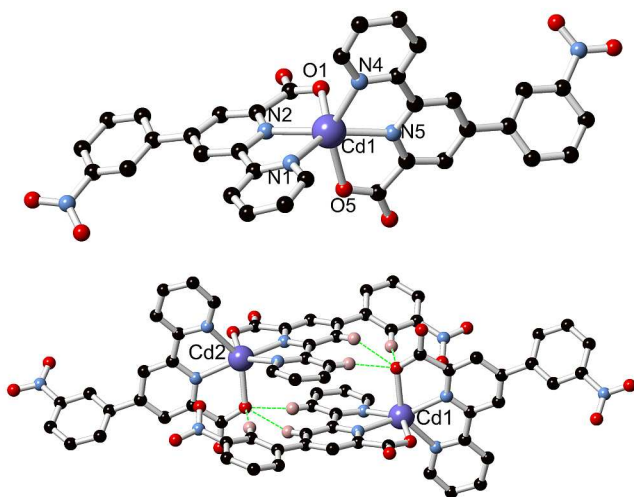
10
11
12
13
14
15 Adjacent complexes in the structure of **1** are linked into pairs by hydrogen bonding through
16 two equivalent lattice water molecules. Non-coordinating carboxylate oxygen atom O2 and
17 coordinating oxygen atom O5 act as acceptors in these interactions, at O \cdots O bond distances
18 2.753(3) and 2.776(3) Å and O-H \cdots O angles of 179.02(13) and 167.55(12)°, respectively. The
19 extended structure of **1** is defined by a series of face-to-face and edge-to-face π - π interactions,
20 and C-H \cdots O hydrogen bonding interactions, forming a densely packed overall structure. Both
21 unique **L1** molecules contain a ‘bay’ of three inwards-directed C-H groups; with each of the
22 groups electron deficient by virtue of attachment to pyridine or nitrophenyl rings, these would be
23 expected to participate in non-classical hydrogen bonding interactions with Lewis basic
24 groups.⁴⁶⁻⁴⁸ In the case of **1**, the two **L1** groups interact with the lattice water molecule O9 and
25 non-coordinating carboxylate oxygen atom O6 through these groups. Each of the C \cdots O distances
26 fall in the range 3.363(3) - 3.598(3) Å, and all six C-H \cdots O angles lie between 139.19(15) -
27 177.87(15) °, indicative of genuine C-H \cdots O hydrogen bonding interactions, and visible on the
28 d_{norm} Hirshfeld surface plot (ESI). The large bipyridyl torsion angle described above may be
29 related to these interactions, particularly those involving the C-H groups at the pyridine 3- and 6-
30 positions.
31
32
33
34
35
36
37
38
39
40
41
42
43
44
45
46
47
48
49
50
51

52
53
54
55 *Structure of [Cd(L2)₂] 2*
56
57
58
59
60

1
2
3 Reacting **L2** with cadmium nitrate under similar conditions to **1** gave colourless crystalline
4 material after 14 hours. Despite screening a wide variety of reaction conditions for the formation
5 of **2**, we consistently obtained small quantities of inorganic impurities alongside the main
6 crystalline product, which were evident both as unexpected Bragg peaks in the PXRD analysis at
7 $2\theta = 10^\circ$, 25° and 50° (Supporting Information), and consistently low values for carbon and
8 nitrogen in microanalysis. These impurities became more prevalent at longer reaction times or
9 with higher temperatures, and most likely correspond to concurrent formation of inorganic
10 cadmium or cadmium formate-based products alongside the major product; such phases are very
11 frequently observed in metal-organic framework syntheses as a result of solvent hydrolysis and
12 redox side-processes.^{49,50}

13
14
15
16
17
18
19
20
21
22
23
24
25
26
27 The diffraction data for $[\text{CdL}_2\text{L}_2]\cdot\text{H}_2\text{O}$ **2** were solved and refined in the orthorhombic space
28 group $Pna2_1$, where the asymmetric unit consists of four unique **L2** ligands deprotonated and
29 coordinated to two unique cadmium(II) ions, each adopting a distorted octahedral N_4O_2
30 coordination sphere (See Figure 2). The four unique N-Cd-O *cis* bite angles lie in the range
31 $70.2(2) - 70.8(2)^\circ$, and similarly the N-Cd-N bite angles are between $70.2(3)$ and $71.4(3)^\circ$,
32 comparing well to complex **1**. Although the octahedral sum of distortion, $\Sigma = 195$ and 193° for
33 Cd1 and Cd2 respectively, resemble that of **1**, the coordination geometries of both cadmium ions
34 display a greater tendency towards trigonal prismatic character (Supporting Information), with
35 trigonal faces defined by the two chelating nitrogen atoms of one **L2** molecule and the
36 coordinating oxygen atom of the other. This assignment is supported by the particularly large *cis*
37 angles between terminal pyridine nitrogen atoms N1, N4, N7 and N10, and the central pyridine
38 nitrogen atoms of opposing ligands N5, N2, N11 and N8, respectively. These angles, which lie in
39 the range $120.6(3) - 132.2(3)^\circ$, help to define flat square faces about the pseudo-trigonal axis.
40
41
42
43
44
45
46
47
48
49
50
51
52
53
54
55
56
57
58
59
60

1
2
3 The related angles in **1**, of 103.66(7) and 118.95(7)°, are much more consistent with the distorted
4 octahedral geometry. All of the coordination bond lengths, falling in the range 2.250(7) -
5 2.373(7) Å, are consistent with those observed in complex **1**, with bonds to the central pyridine
6 nitrogen atoms displaying the shortest distances. Unlike **1**, all of the pyridine-pyridine torsions in
7
8 **2** are near planarity (in the range 5.3(9) – 7.8(9) °), and the phenyl-pyridyl torsion angles display
9
10 comparable values, in the range 15.7(11) – 49.1(10)°.
11
12
13
14
15
16
17



18
19
20
21
22
23
24
25
26
27
28
29
30
31
32
33
34
35
36
37
38
39
40
41
42
43
44
45
46
47
48
49
50
51
52
53
54
55
56
57
58
59
60
Figure 2 Structure of complex **2**, with labelling scheme for coordinating atoms (top) and showing polydentate C-H···O hydrogen bonding interactions between adjacent complexes in the extended structure (bottom). Selected hydrogen atoms are omitted for clarity.

Two predominant intermolecular interaction modes are present between complexes within the structure of **2**. Non-equivalent pairs of complexes associate with face-to-face π - π interactions between the two dipyridyl groups, with (dipyridyl-dipyridyl) mean interplanar angle of 2.2° and minimum interatomic distance of 3.250(12) Å (C4-C40). These interactions are supplemented by reciprocated chelating C-H···O hydrogen bonding interactions between the inwards-directed C-H groups of each ring on one complex and the coordinating carboxylate oxygen atom (O5/O9) of

1
2
3 the adjacent species. For the tightly bound dimers, the six C-H \cdots O interactions display C \cdots O
4 distances in the range 3.247(10) - 3.576(11) Å, and C-H \cdots O angles 148.8(6) - 171.0(5)°. These
5 interactions are also a dominant feature on the calculated Hirshfeld surface (ESI).^{51,52}
6
7
8 Additionally, the dimeric association of neighbouring complexes leads to unusually close
9 contacts between the nitro groups and the chelating pyridine nitrogen atoms of the adjacent
10 ligand, with N \cdots O distances 2.793(10) and 2.932(11) for O3 \cdots N11 and O15 \cdots N5, respectively.
11
12
13 These dimeric assemblies are further linked to neighbouring complexes by weaker C-H \cdots O
14 hydrogen bonding interactions to non-coordinating carboxylate oxygen atoms, although the
15 influence of this interaction on the extended structure is lessened by the lack of any substantial π -
16 π overlap between the adjacent complexes. Additionally, various C-H \cdots O interactions involving
17 the nitro groups, and C-H \cdots π interactions are present within the structure, contributing to a
18 densely packed extended structure containing no void volume or encapsulated solvent molecules.
19
20
21
22
23
24
25
26
27
28
29
30
31
32
33

34 **Synthesis of polynuclear Cd complexes**

35
36 *[Cd₃(L1)₃(NO₃)₂(DMF)₄]NO₃ 3 and [Cd₃(L2)₃(NO₃)₂(DMF)₄]NO₃ DMF 4*

37
38
39 Interestingly, during the screening process for the optimised syntheses of **1** and **2**, two
40 additional phases were discovered. Reacting either **EtL1** or **HL2** with cadmium nitrate at higher
41 concentrations in pure DMF and 1:1 M:L stoichiometries gave rise to a different crystalline
42 material (in both cases) compared to those observed in **1** and **2**. The single crystal X-ray
43 diffraction data of [Cd₃(L1)₃(NO₃)₂(DMF)₄]NO₃ **3** were solved and refined in the triclinic space
44 group *P*-1, with the asymmetric unit containing three unique **L1** ligands, deprotonated and
45 coordinating to three unique Cd^{II} ions, forming a trinuclear complex. Each cadmium ion adopts a
46 seven-coordinate pentagonal bipyramidal geometry. The two axial positions of each metal ion
47
48
49
50
51
52
53
54
55
56
57
58
59
60

1
2
3 are occupied by either nitrate anions or DMF molecules, while the equatorial positions are
4
5 occupied by a single tridentate chelate from one molecule of **L1** and a chelating carboxylate
6
7 group from another **L1** molecule; each ligand coordinates in a μ_2 - $\kappa N,N',O:\kappa O,O'$ bridging mode
8
9 (Figure 3). The overall assembly resembles an approximately threefold-symmetric disc with a
10
11 central six-membered Cd_3O_3 ring, with the three $Cd\cdots Cd$ distances 4.819(1), 4.686(1) and
12
13 4.6745(9) Å for Cd_3 - Cd_2 , Cd_2 - Cd_1 and Cd_1 - Cd_3 , respectively. This approximate symmetry is
14
15 disrupted by the unsymmetric distribution of the axial ligands, where cadmium ion Cd_3 has both
16
17 axial positions occupied by DMF molecules, while Cd_1 and Cd_2 are coordinated by one nitrate
18
19 and one DMF ligand each, in an *anti* arrangement to one another across the central plane. For
20
21 charge balance, the asymmetric unit also contains one disordered non-coordinating nitrate anion,
22
23 while no non-coordinating solvent molecules were detected crystallographically. All of the
24
25 metal-ligand bond distances are greater in **3** than their equivalents in the related mononuclear
26
27 complex **1**, falling in the range 2.299(7) – 2.353(6) Å for Cd-N bonds and 2.289(7) – 2.507(6) Å,
28
29
30
31
32
33
34 consistent with the higher coordination number of the metal ions in **3**.
35
36
37
38
39
40
41
42
43
44
45
46
47
48
49
50
51
52
53
54
55
56
57
58
59
60

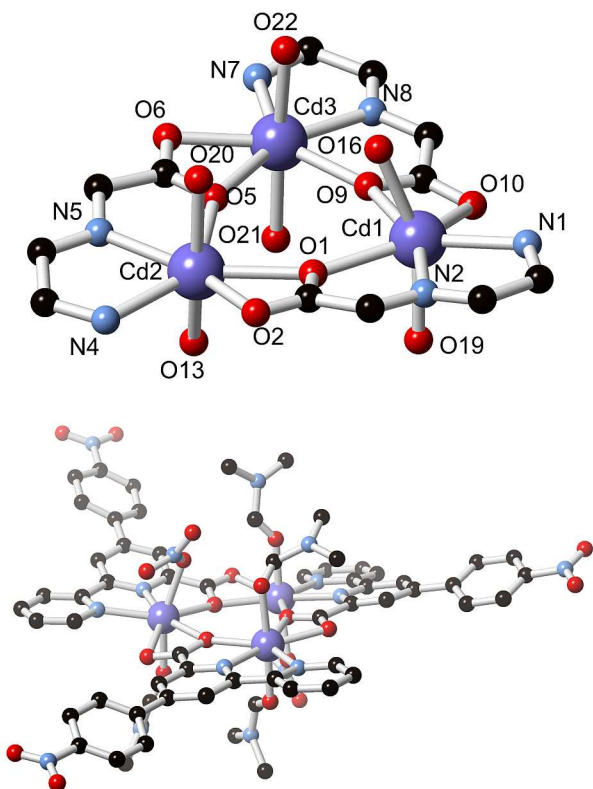


Figure 3 Structure of complex **3**, showing the central cluster core and coordination environment with labels for coordinating atoms (top) and the complete structure of the complex (bottom). Non-coordinating nitrate anion and all hydrogen atoms are omitted for clarity.

The largely flat trinuclear clusters in **3** associate through various face-to-face π - π interactions, supported by C-H \cdots O interactions between the **L1** backbone and the nitrate and DMF ligands of adjacent complexes. These interactions are generally reminiscent of those observed in the structures of the two mononuclear complexes. In addition, the bridging coordination geometry provides additional opportunities for chelated C-H \cdots O interactions on the outer faces of each **L1** molecule in concert with the outer pyridine C-H groups of adjacent ligands. The extended structure of **3** can be considered in terms of columns aligned parallel to the crystallographic *a* axis consisting of the central metal cores and axial ligands, with the disc-shaped periphery of **L1**

1
2
3 groups extending into the *b* and *c* directions and interdigitated with those of adjacent columns,
4 supported by π - π and C-H \cdots O interactions. These columns are arranged in a honeycomb rod
5 packing motif, with the interstitial spaces occupied by the disordered nitrate anions.
6
7
8
9

10
11
12 The reaction of **HL2** with cadmium nitrate under similar conditions to **3** gave colourless
13 crystals of $[\text{Cd}_3(\text{L2})_3(\text{NO}_3)_2(\text{DMF})_4]\text{NO}_3 \cdot \text{DMF} **4**, the diffraction data for which were solved and
14 refined in the triclinic space group *P*-1. The asymmetric unit of **4** is closely related to that of **3**,
15 containing a trinuclear complex consisting of three seven-coordinate pentagonal bipyramidal Cd^{II}
16 ions, three deprotonated **L2** ligands, four DMF and two nitrate ligands, and a non-coordinating
17 nitrate anion and lattice DMF molecule. The three cadmium ions and ligand molecules in **4** adopt
18 equivalent coordination geometries to those in **3**, and the Cd-Cd distances in the range 4.5999(7),
19 - 4.8394(6) Å are in close agreement with those observed in **3**. The arrangement of nitrate and
20 DMF ligands in **4** is slightly different, with both nitrate ligands occupying the axial positions of
21 cadmium ion Cd_2 , while the coordination spheres of the other two cadmium ions are completed
22 by DMF ligands only. No meaningful differences in metal-ligand bond lengths are observed
23 between the three cadmium ions, or with the equivalent distances in the structure of **3**.
24
25
26
27
28
29
30
31
32
33
34
35
36
37
38
39
40
41
42
43
44
45
46
47
48
49
50
51
52
53
54
55
56
57
58
59
60$

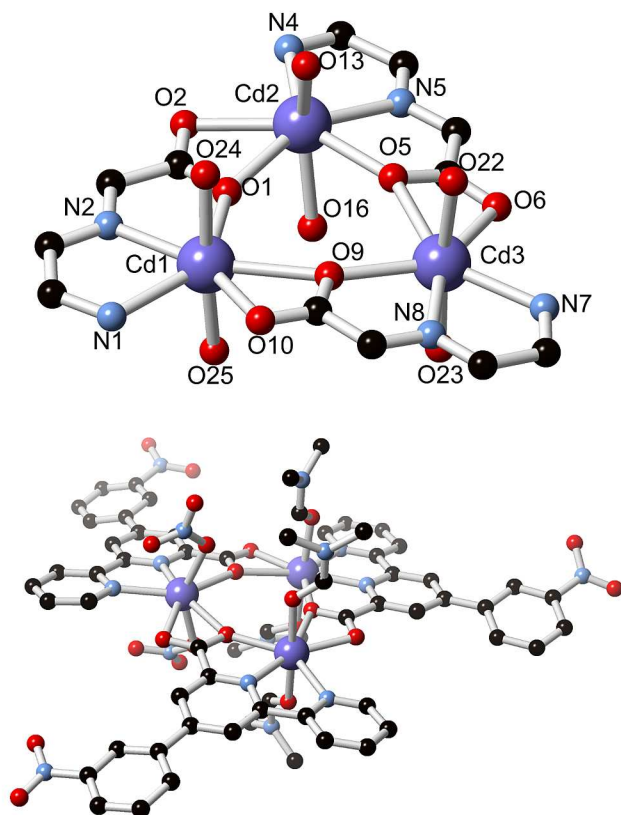
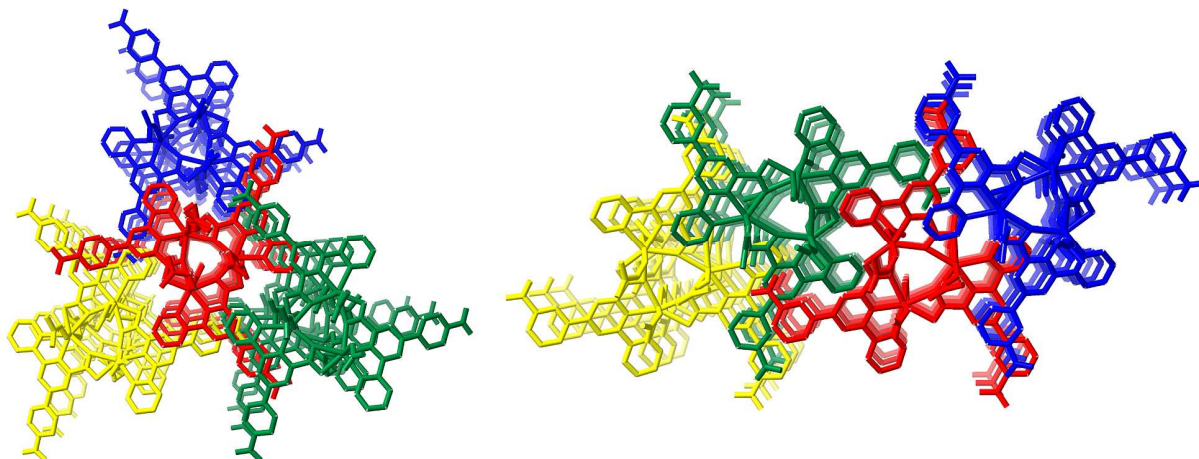


Figure 4 Structure of complex **4**, showing core connectivity with labelling scheme for coordinating atoms (top) and complete structure of the complex (bottom). Non-coordinating DMF molecule and nitrate anion, positional disorder in coordinating DMF ligand, and all hydrogen atoms are omitted for clarity.

Adopting a similar disc-like shape, the intermolecular interactions in the structure of **4** are also related to those observed in **3**. The packing motifs are largely dominated by π - π interactions, augmented by C-H \cdots O interactions between the electron deficient aromatic C-H groups and the oxygen atoms of axial ligands from adjacent molecules. Numerous such interactions can be expressed in the Hirshfeld surface with mapped d_{norm} plot for the complex (Supporting Information), and features on the fingerprint plot reminiscent of **3** and the mononuclear complexes **1** and **2** are present (See discussion section). As was the case in **3**, adjacent complexes

1
2
3 overlap along the *a* axis into columns which interdigitate with one another *via* these interactions.
4
5 However, rather than the regular honeycomb packing motif of these columns observed in **3**, in **4**
6
7 these columns are arranged into layers oriented in the *ac* plane by intermolecular π - π and C-
8
9 H \cdots O interactions, while the interactions in the *b* direction separate the metal sites by a greater
10
11 degree.
12
13



14
15
16
17
18
19
20
21
22
23
24
25
26
27
28
29
30
31
32 **Figure 5** Comparison in the extended packing motif for complexes **3** (left) and **4** (right); while
33
34 a single stack of **3** interacts with three others in a pseudo-trigonal packing arrangement, stacks of
35
36 **4** associate into dimers at the *anti-anti* edge before further associating (*c* axis horizontal).
37
38

39
40
41 Interestingly, both complexes **3** and **4** exhibited sensitivity to atmospheric water on extended
42
43 drying in ambient air. Thermogravimetric analysis was conducted on two batches of **3** and **4**, one
44
45 of which was freshly synthesised whereas the other had been exposed to air for 3 weeks. The
46
47 freshly isolated samples both exhibit small initial mass losses (*ca.* 4%) corresponding to surface
48
49 and loosely bound solvent, plus mass losses in the temperature range 100-230 °C corresponding
50
51 to loss of the coordinating and non-coordinating DMF molecules (measured 14% and 16%,
52
53 calculated 16% and 19% for **3** and **4**, respectively). On standing in air for three weeks, the higher
54
55
56
57
58
59
60

1
2
3 temperature steps (100 - 230 °C) are reduced to 4% and 8% for **3** and **4**, respectively, while both
4
5 compounds exhibit an increased 8% mass loss between room temperature and 100 °C. The loss
6
7 of lattice DMF molecules and incorporation of atmospheric water in both cases is corroborated
8
9 by microanalysis on the air-dried samples, which showed both compounds can be described by
10
11 the formulation $[\text{Cd}_3(\text{L})_3(\text{NO}_3)_3] \cdot 1.5\text{DMF} \cdot 3\text{H}_2\text{O}$ (calculated 6.5% wt. DMF, 3 % wt. H_2O), but
12
13 not suitably approximated by the original loading of 4-5 DMF molecules per cluster. Adsorption
14
15 of atmospheric water is often observed in both polymeric frameworks and porous molecular
16
17 materials, and can lead to structural changes particularly where the guest molecules are loosely
18
19 bound or arranged in contiguous solvent channels.⁵³⁻⁵⁵ Exposure to air for extended periods led to
20
21 cracking and consequent loss of single crystallinity in both **3** and **4**, preventing the monitoring of
22
23 this process by X-ray diffraction. Analysis by PXRD of the dried sample shows degradation of
24
25 the original Bragg peaks but the emergence of no new peaks in the pattern, suggesting a loss of
26
27 crystallinity rather than a transition to a new crystalline phase (Supporting Information)
28
29
30
31
32
33
34
35
36
37
38

39 **Synthesis and structure of Co^{II} and Co^{III} complexes of L1 and L2**

40
41 After the examination of the coordination chemistry of **L1** and **L2** with the labile coordination
42
43 sphere of Cd^{II} , and the emergence of both mononuclear and trinuclear species for each ligand, we
44
45 turned our attention to Co^{II} , with the expectation of forming more well-defined mononuclear
46
47 complexes with regular octahedral geometry. Surprisingly, however, the reaction between either
48
49 **EtL1**, **HL1** or **HL2** in DMF at 100 °C gave mixtures of products after 24 hours. The
50
51 predominant products were the divalent species $[\text{Co}(\text{L1})_2]$ **5** and $[\text{Co}(\text{L2})_2]$ **7**, however a
52
53 crystalline trivalent impurity was identified in both cases, with the formulation $[\text{Co}(\text{L1})_2]\text{NO}_3$ **6**
54
55
56
57
58
59
60

1
2
3 or [Co(L2)₂]NO₃ **8**. Although such *in-situ* metal ion oxidations under solvothermal conditions are
4
5 not especially uncommon,⁵⁶ we were unable to generate either trivalent species on larger scales
6
7 or as a pure phase. Nonetheless, modifying the reaction solvent to 1:1 H₂O/DMF was adequate to
8
9 remove the trivalent impurity from the isolated material and generate each of the divalent
10
11 materials as crystalline phases in sufficient quantity to conduct the necessary analysis to both
12
13 asses the purity and fully characterise the complexes.
14
15
16
17
18
19

20 *Structure of [Co(L1)₂] 5 and [Co(L1)₂]NO₃ 6*

21
22
23
24

25 The diffraction data for **5** were solved and refined in the monoclinic space group *C2/c*, with the
26
27 asymmetric unit containing one molecule of **L1**, deprotonated and coordinating to a Co^{II} ion
28
29 occupying a crystallographic special position. Two equivalent ligand molecules coordinate to the
30
31 cobalt ion in a distorted octahedral geometry, with each ligand providing narrow *cis* bite angles
32
33 of 76.95(13)° and 75.42(14)° for O1-Co1-N2 and N1-Co1-N2, respectively. These angles are
34
35 comparable to those observed in the mononuclear complexes **1** and **2**, although the octahedral
36
37 distortion parameter Σ of 132° is considerably smaller, consistent with the greater tendency
38
39 towards regular octahedral geometry for the d⁷ Co^{II} ion compared to the d¹⁰ Cd^{II} ion. The metal-
40
41 ligand bond lengths also show some level of distortion, with the Co-N bond to the central
42
43 pyridine nitrogen atom N1 of 2.041(2) Å considerably shorter than the bonds to N2 and O1, at
44
45 2.142(5) and 2.114(4) Å, respectively. The ligand adopts a relatively planar conformation, with a
46
47 slight twist in the nitrophenyl ring relative to the central pyridine ring of 29.9(7) ° (C9-C8-C12-
48
49 C17 dihedral angle).
50
51
52
53
54
55
56
57
58
59
60

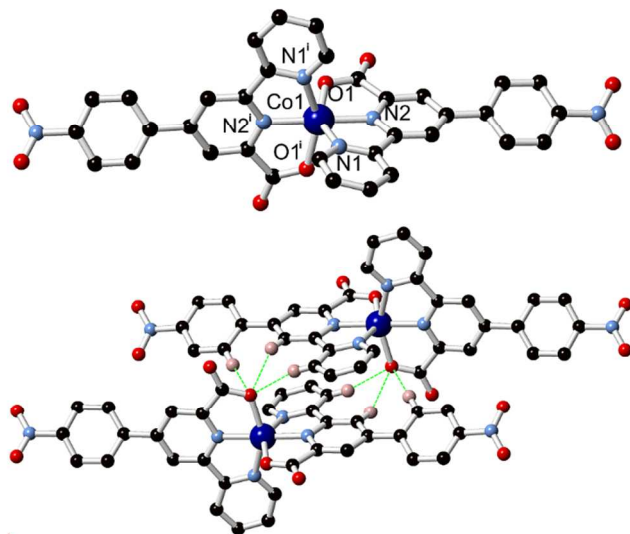


Figure 6 Structure of complex **5**, with labelling scheme for coordinating atoms (top) and reciprocated polydentate C-H \cdots O interactions between adjacent molecules in the extended structure (bottom). Symmetry codes used to generate equivalent atoms: (i) 1-x, +y, $\frac{1}{2}$ -z.

Adjacent molecules of **5** associate through a π - π stacking interaction coupled with a series of C-H \cdots O interactions. The dipyriddy moieties from two molecules associate in an offset face-to-face fashion, with mean interplanar distance 3.40 Å between parallel dipyriddy units. This interaction places the coordinating carboxylate oxygen atom O1 in the vicinity of several electron deficient C-H groups from the adjacent molecule, with C \cdots O distances 3.422(5), 3.270(5) and 3.670(5) Å and C-H \cdots O angles 152.5(3), 161.0(3) and 156.0(3) $^\circ$ for C7, C4 and C13, respectively. These interactions, similar to those observed for complex **2**, and which are a dominant feature on the calculated Hirshfeld surface for the molecule (ESI), are reciprocated between pairs of molecules, and align complexes into columns parallel to the *c* axis. Adjacent columns associate through weaker π - π and C-H \cdots π interactions involving the terminal nitrophenyl group.

1
2
3
4
5
6
7
8
9
10
11
12
13
14
15
16
17
18
19
20
21
22
23
24
25
26
27
28
29
30
31
32
33
34
35
36
37
38
39
40
41
42
43
44
45
46
47
48
49
50
51
52
53
54
55
56
57
58
59
60

The diffraction data for the trivalent species $[\text{Co}(\text{L1})_2]\text{NO}_3$ **6** was refined in the triclinic space group $P\bar{1}$, with the asymmetric unit containing one $[\text{Co}(\text{L1})_2]^+$ cation and an associated non-coordinating nitrate anion. The geometry of the complex is closely related to that observed in **5**, with the expected contraction in M-L bond lengths, each of which is shortened by *ca.* 0.1 Å compared to the divalent complex. Again, the bonds to the central pyridine rings (1.855(2) and 1.857(2) Å for N2 and N5, respectively) are shorter than those to the outer pyridine groups (1.943(2) and 1.959(2) Å for N1 and N2, respectively) and the carboxylate oxygen atoms (1.931(2) and 1.913(2) Å for O1 and O5, respectively). The octahedral distortion parameter is also significantly reduced to 63°, consistent with a better fit of the smaller Co^{III} ion within the binding pocket.

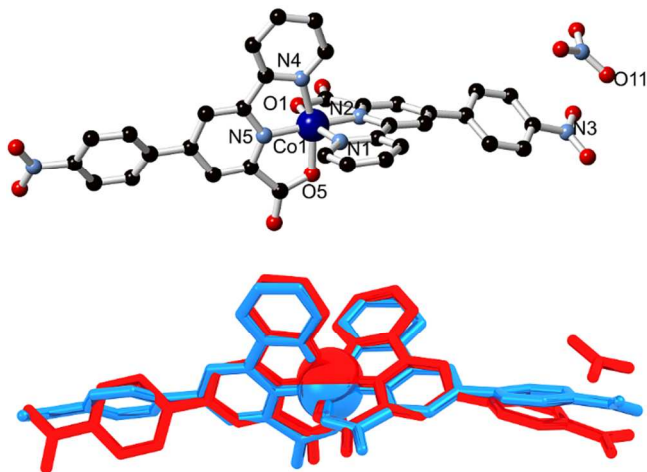


Figure 7 Structure of complex **6** with partial atom labelling scheme (Top), and overlaid structures of complex **5**, shown in blue, and complex **6**, shown in red (bottom). Hydrogen atoms are omitted for clarity. The distance $\text{N3}\cdots\text{O11}$ corresponding to the anion $\cdots\pi$ -hole contact is 2.873(3) Å.

1
2
3 The intermolecular interactions of **6** are related to those observed in **5**, with variations based on
4 slight differences in ligand geometry and the presence of the nitrate anion within the lattice. One
5 unique **L1** group engages in a similar π - π stacking/C-H \cdots O hydrogen bonding mode as observed
6 in **5**, albeit with considerably weaker inter-complex interactions. The mean interplanar distance
7 of 3.52 Å between the equivalent dipyriddy mean planes and C \cdots O distances in the range
8 3.430(3) – 4.306(3) Å for this interaction are both indicative of a significantly weaker attractive
9 force between the two molecules. The other **L1** molecule interacts with the nitrate anion through
10 an unusually short electrostatic interaction between nitrate oxygen atom O11 and nitrogen atom
11 N3 from the aromatic nitro group, of N-O distance 2.873(3) Å. In similar systems this anion- π
12 interaction is accounted for by the presence of a nitroaromatic π -hole.⁵⁷⁻⁵⁹ This interaction is
13 accompanied by a substantial bending of the phenyl ring of the **L1** molecule out of the
14 meridional plane of the metal centre in the opposite direction from the nearby anion. The
15 differences in geometry can be conveniently visualised by overlaying the two molecular
16 structures (Figure 7). The interplanar angle of 12.0° between the nitrate mean plane and the mean
17 plane of the aromatic nitro group C-NO₂ shows the two group are near-parallel to each other.
18 Besides these interactions, the extended structure is densely packed, with no encapsulated
19 solvent molecules or void volume, and is largely defined by a series of C-H \cdots O interactions
20 involving the nitrate anion, and additional C-H \cdots π interactions of the terminal phenyl ring.
21
22
23
24
25
26
27
28
29
30
31
32
33
34
35
36
37
38
39
40
41
42
43
44
45
46
47

48 *Structure of [Co(L2)₂] 7 and [Co(L2)₂]NO₃ 8*

49
50
51
52

53 **L2** was reacted with cobalt nitrate hexahydrate in DMF at 100 °C to yield light brown
54 crystalline material after 24 hrs, which contained a mixture of the divalent [Co(L2)₂] **7** and the
55
56
57
58
59
60

1
2
3 trivalent $[\text{Co}(\text{L2})_2]\text{NO}_3$ **8**. Although the crystalline material of **7** was not of sufficient quality to
4 analyse by single crystal X-Ray diffraction, the X-ray powder diffraction pattern of **7** closely
5 matched the structurally equivalent Cd monomer $[\text{Cd}(\text{L2})_2]$ **2**, and microanalysis confirmed an
6 equivalent formulation as the divalent anhydrate $[\text{Co}(\text{L2})_2]$. The single crystal X-ray diffraction
7 data for $[\text{Co}(\text{L2})_2]\text{NO}_3$ were solved and refined in the monoclinic space group $P2_1/n$ where the
8 asymmetric unit contains two molecules of **L2** deprotonated and coordinating to a Co^{III} ion, and
9 an associated non-coordinating nitrate anion. Compound **8** displays very similar structural
10 features to those seen in **6**. A similar distorted octahedral geometry is observed with comparable
11 *cis* bite angles at $85.59(12)^\circ$ and $83.32(12)^\circ$ for O1-Co1-N2 and N1-Co1-N5, respectively, and
12 $81.99(12)^\circ$ and $81.84(13)^\circ$ for N1-Co1-N2 and N4-Co1-N5, respectively. The distortion
13 parameter Σ of 70° is also similar to that seen in **6**. Also similar are the M-L bond lengths,
14 wherein the bonds to the outer pyridine rings ($1.948(3)$ and $1.953(3)$ Å for N1 and N4
15 respectively) are longer than those to the central groups ($1.847(3)$ and $1.856(3)$ Å for N2 and N5
16 respectively) and the carboxylate atoms ($1.918(3)$ and $1.919(3)$ Å for O5 and O1 respectively).
17 In corroboration with **6** the nitrate anion enforces a break in the ligand symmetry, but **8** shows
18 significantly less π - π stacking than in the 4-nitro analogue.
19
20
21
22
23
24
25
26
27
28
29
30
31
32
33
34
35
36
37
38
39
40
41
42
43
44
45
46
47
48
49
50
51
52
53
54
55
56
57
58
59
60

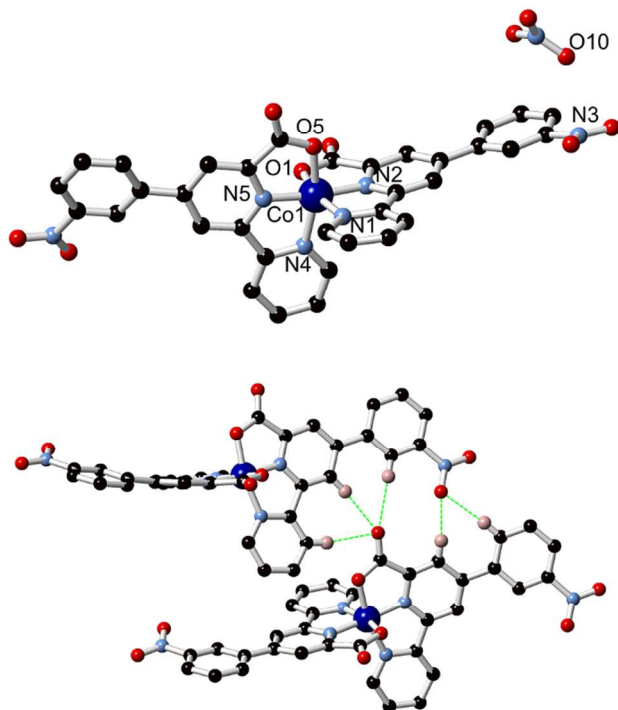


Figure 8 Structure of complex **8** with partial atom labelling scheme (Top), and polydentate C-H \cdots O hydrogen bonding interactions between adjacent molecules in the structure of **8** (Bottom). Selected hydrogen atoms are omitted for clarity. The distance N3 \cdots O10 is 2.819(4) Å.

The presence of the nitro group in the 3- position affords the opportunity for extended C-H \cdots O hydrogen bonding, with pairs of complexes linked by an interaction consisting of 5 HB donors and 2 HB acceptors. Oxygen atom O3 from the 3-NO₂ group accepts two hydrogen bonds from the carbon atoms C25 and C34 of the adjacent molecule, with C \cdots O distances 3.196(4) and 3.479(5) Å and C-H \cdots O angles of 171.1(2) and 160.0(2) ° respectively. Carbon atoms C7 and C13 act as hydrogen bond donors to the non-coordinating carboxylate oxygen atom O6, at C \cdots O distances 3.351(4) and 3.454(4) Å and C-H \cdots O angles 172.2(2) and 166.4(2)°, respectively. Carbon atom C4 also participates in C-H \cdots O hydrogen bonding primarily with the non-

1
2
3 coordinating oxygen atom O6 at C \cdots O distance 3.513(5) Å and a C-H \cdots O angle of 169.2 (2)°
4
5 and is weakly bifurcated by the coordinating oxygen atom O5 (C \cdots O distance 3.194(5) Å and C-
6
7 H \cdots O angle 133.7(3)°).
8
9

10
11
12 In addition to these interactions linking adjacent complexes, several electrostatic contacts
13 are observed between the complex and the nitrate anion. Carbon atom C1 donates a weak
14 hydrogen bond to nitrate oxygen atom O11, at C \cdots O distance 3.194(5) Å and C-H \cdots O angle
15
16 157.5(2) °. Similarly to **2**, a short intermolecular anion \cdots π -hole contact is observed between the
17
18 nitrate anion and one aromatic nitro group. The distance between nitrate oxygen atom O10 and
19
20 nitro group nitrogen atom N3 of 2.819(4) Å is marginally shorter compared to **6**, while the
21
22 nitrate-nitroaryl mean interplanar angle of 52° is significantly larger.
23
24
25
26
27
28
29
30
31

32 Discussion

33
34 The combination of electron-deficient pyridine and nitrophenyl groups makes **L1** and **L2**
35 prime candidates as C-H hydrogen bond donors, which are well known to play a significant role
36 in crystal packing, especially when present in the absence of stronger directional intermolecular
37
38 synthons.⁴⁶⁻⁴⁸ In each of the 7 complexes described above, these interactions are prevalent and
39 particularly occur between the three inwardly directed C-H groups from the 3 aromatic rings (the
40
41 6', 3 and 3''/2'' positions for **L1** and **L2**, respectively) and the carboxylate oxygen atoms of an
42
43 adjacent complex. The particular interaction modes of the ML₂ complexes presented above also
44
45 include contributions from face-to-face π - π interactions, and are reminiscent of the well-known
46
47 P4AE interaction mode reported by Dance which is prevalent in many octahedral metal
48
49 complexes and for ligands containing predominantly aromatic character.^{60,61} The C-H \cdots O
50
51
52
53
54
55
56
57
58
59
60

1
2
3 character of the interactions in complexes **1** – **6** and **8** (where **7** is presumed to behave in a very
4 similar fashion to **2** by virtue of their equivalent cell settings) can be summarised with the use of
5 the Hirshfeld surface fingerprint plot, highlighting O···H and H···O contacts within the
6 structures (Figure 9).^{51,52} In each case, well-defined and symmetric features consistent with
7 reciprocated C-H···O interactions between complexes are observed, which also appear as notable
8 features on the Hirshfeld surface plots mapped with the d_{norm} function for each complex
9 (Supporting Information). The asymmetric contact for complex **1** represents the additional strong
10 O-H···O hydrogen bond from the lattice water molecule.
11
12
13
14
15
16
17
18
19
20
21

22 The emergence of multiple crystalline phases from each combination of metal and ligand is a
23 commonly encountered obstacle in the solvothermal preparation of metal complexes and
24 coordination polymers, where polymorphism or co-existing isomeric species are regularly
25 observed.^{62,63} In the instances reported above, single phase products for **1**, **3**, **4**, **5** and **7** could be
26 generated by careful and systematic exploration of the reaction conditions, while complex **2** was
27 observed to co-crystallise with small quantities of inorganic impurities under all reaction
28 conditions. The trivalent cobalt species **6** and **8** could not be generated in bulk, presumably due
29 to the consumption of the trace oxidant present in the reaction mixture (potentially either
30 atmospheric oxygen or a nitrate-derived species) and the concomitant build-up of reduced by-
31 products. Nonetheless, the addition of stoichiometric nitric acid had no effect on the outcome of
32 the reaction, indicating the significant stability of the divalent species once formed.
33
34
35
36
37
38
39
40
41
42
43
44
45
46
47
48
49
50
51
52
53
54
55
56
57
58
59
60

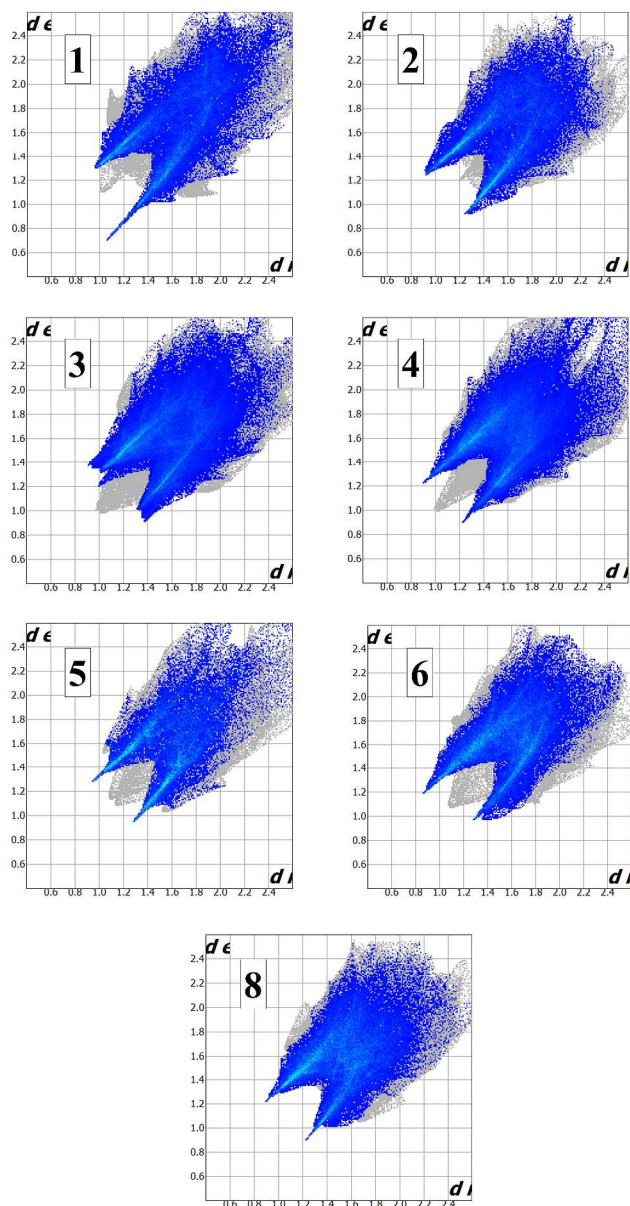


Figure 9 Hirshfeld surface fingerprint plots for complexes **1-6** and **8** with $\text{H}\cdots\text{O}$ and $\text{O}\cdots\text{H}$ contacts highlighted, with each plot showing the distinctive symmetric binodal pattern indicative of directional intermolecular interactions.

Conclusions

We have prepared and structurally characterised 8 new crystalline *d*-block metal complexes of the *N,N,O*-terdentate ligands 4-(4-nitrophenyl)-2,2'-bipyridine-6-carboxylate **L1** and 4-(3-nitrophenyl)-2,2'-bipyridine-6-carboxylate **L2**, using solvothermal synthesis techniques including *in-situ* ester hydrolysis to generate single-phase products. In the case of the cadmium(II) complexes **1** – **4**, modification of the synthesis conditions (stoichiometry, temperature and reaction time) gave either mononuclear complexes **1** or **2**, or trinuclear clusters **3** or **4**. In the case of cobalt(II)/(III) mononuclear complexes were exclusively observed, with the divalent compounds **5** and **7** including trace amounts of trivalent compounds **6** and **8**, respectively, which could subsequently be eliminated by modifying the reaction solvent. In all of the complexes, the extended structures were strongly influenced by C-H \cdots O interactions between the electron deficient aromatic backbone of the ligand and carboxylate oxygen atoms of adjacent complexes, in a readily identifiable polydentate intermolecular interaction motif. With an understanding of the fundamental structural and coordination chemistry now in hand, these results provide the background for development of the highly modular 6-carboxy-4-aryl-2,2'-bipyridine building block as a robust coordinating tecton in larger *d*-block metallosupramolecular assemblies.

Acknowledgements

The authors gratefully acknowledge Science Foundation Ireland (SFI PI Awards 10/IN.1/B2999 and 13/1A/1865 to TG), the Irish Research Council (IRC, GOIPD/2015/446 to CSH) and the School of Chemistry, Trinity College Dublin for financial support (Postgraduate Studentship to HLD). We thank Drs. John O'Brien, Brendan Twamley and Martin Feeney (TCD) for instrumental and technical assistance.

Supporting Information. Thermogravimetric analysis plots, X-ray powder diffraction patterns, ORTEP-style crystallographic figures, full NMR spectra and Hirshfeld surface plots and additional figures. This material is available free of charge via the Internet at <http://pubs.acs.org>. See DOI: 10.1039/x0xx00000x. CCDC 1544479-1544485

Corresponding Author

Email: gunnlaut@tcd.ie

Author Contributions

The manuscript was written through contributions of all authors. All authors have given approval to the final version of the manuscript.

References

1. Kolesnichenko, I. V.; Anslyn, E. V. *Chem. Soc. Rev.* **2017**, *46*, 2385-2390.
2. Martinez-Calvo, M.; Kotova, O.; Möbius, M. E.; Bell, A. P.; McCabe, T.; Boland, J. J.; Gunnlaugsson, T. *J. Am. Chem. Soc.* **2015**, *137*, 1983-1992.
3. Byrne, J. P.; Martinez-Calvo, M.; Peacock, R. D.; Gunnlaugsson, T. *Chem. Eur. J.* **2016**, *22*, 486-490.
4. Kitchen, J. A. *Coord. Chem. Rev.* **2017**, *340*, 232-246.
5. Byrne, J. P.; Kitchen, J. A.; Gunnlaugsson, T. *Chem. Soc. Rev.* **2014**, *43*, 5302-5325.
6. Cook, T. R.; Zheng, Y.-R.; Stang, P. J. *Chem. Rev.* **2013**, *113*, 734-777.
7. Lifschitz, A. M.; Rosen, M. S.; McGuirk, C. M.; Mirkin, C. A. *J. Am. Chem. Soc.* **2015**, *137*, 7252-7261.
8. Kotova, O.; Daly, R.; dos Santos, C. M. G.; Kruger, P. E.; Boland, J. J.; Gunnlaugsson, T. *Inorg. Chem.* **2015**, *54*, 7735-7741.
9. McCarney, E. P.; Hawes, C. S.; Blasco, S.; Gunnlaugsson, T. *Dalton Trans.* **2016**, *45*, 10209-10221.
10. Kaes, C.; Katz, A.; Hosseini, M.W. *Chem. Rev.* **2000**, *100*, 3553-3590.
11. Schubert, U.S.; Eschbaumer, C. *Angew. Chem. Int. Ed. Engl.* **2002**, *41*, 2892-2926.

- 1
2
3
4
5
6
7
8
9
10
11
12
13
14
15
16
17
18
19
20
21
22
23
24
25
26
27
28
29
30
31
32
33
34
35
36
37
38
39
40
41
42
43
44
45
46
47
48
49
50
51
52
53
54
55
56
57
58
59
60
12. Yum, J.-H.; Baranoff, E.; Kessler, F.; Moehl, T.; Ahmad, S.; Bessho, T.; Marchioro, A.; Ghadiri, E.; Moser, J.-E.; Yi, C.; Nazeeruddin, M. K.; Grätzel, M. *Nature Commun.* **2012**, *3*, 631.
 13. Prier, C. K.; Rankic, D. A.; MacMillan, D. W. C. *Chem. Rev.* **2013**, *113*, 5322-5363.
 14. Sakamoto, R.; Wu, K.-H.; Matsuoka, R.; Maeda, H.; Nishihara, H. *Chem. Soc. Rev.* **2015**, *44*, 7698-7714.
 15. Auböck, G.; Chergui, M. *Nature Chem.* **2015**, *7*, 629-633.
 16. Szczerba, W.; Schott, M.; Riesemeier, H.; Thünemann, A. F.; Kurth, D. G. *Phys. Chem. Chem. Phys.* **2014**, *16*, 19694-19701.
 17. Berg, K.E.; Tran, A.; Raymond, M.K.; Abrahamsson, M.; Wolny, J.; Redon, S.; Andersson, M.; Sun, L.; Styring, S.; Hammarström, L.; Toftlund, H.; Åkermark, B. *Eur. J. Inorg. Chem.*, **2001**, 1019-1029.
 18. Eicher, T.; Hauptmann, S. *The Chemistry of Heterocycles*, 2nd Ed., Wiley-VCH, Weinheim, 2003.
 19. Norris, M. R.; Concepcion, J. J.; Glasson, C. R. K.; Fang, Z.; Lapidés, A. M.; Ashford, D. L.; Templeton, J. L.; Meyer, T. J. *Inorg. Chem.* **2013**, *52*, 12492-12501.
 20. Kelly, N. R.; Goetz, S.; Hawes, C. S.; Kruger, P. E. *Tetrahedron Lett.* **2011**, *52*, 995-998.
 21. J.-C. G. Bunzli, L. J. Charbonniere and R. F. Ziessel, *J. Chem. Soc. Dalton. Trans.* **2000**, 1917-1923.

- 1
2
3 22. Ryan, G.J.; Elmes, R.B.P.; Quinn, S.J.; Gunnlaugsson, T, *Supramol. Chem.* **2012**, *24*, 175-
4 188.
5
6
7
8
9 23. Kopchuk, D.S.; Krinochkin, A.P.; Kozhevnikov, D.N.; Slepukhin, P.A. *Polyhedron* **2016**,
10 *118*, 30-36.
11
12
13
14 24. Tynan, E.; Jensen, P.; Kelly, N. R.; Kruger, P. E., Lees, A. C.; Nieuwenhuyzen, M. *Dalton*
15 *Trans.* **2003**, 1223-1228.
16
17
18
19
20 25. Chen, J.-L.; Fu, X.-F.; Wang, J.-Y.; Guo, Z.-H.; Xiao, Y.-L.; He, L.-H.; Wen, H.-R. *Inorg.*
21 *Chem. Commun.* **2015**, *53*, 88-91.
22
23
24
25
26 26. Norrby, T.; Börje, A.; Åkermark, B.; Hammarström, L.; Alsins, J.; Lashgari, K.;
27 Norrestam, R.; Mårtensson, J.; Stenhagen, G. *Inorg. Chem.* **1997**, *36*, 5850-5858.
28
29
30
31 27. Goodwin, H. A.; Sylva, R. N. *Aust. J. Chem.* **1967**, *20*, 217-225.
32
33
34 28. Sylva, R. N.; Goodwin, H. A.; *Aust. J. Chem.* **1969**, *22*, 2013-2016.
35
36
37
38 29. Akerboom, S.; van den Elshout, J. J. M. H.; Mutikainen, I.; Siegler, M. A.; Fu, W. T.;
39 Bouwman, E *Eur. J. Inorg. Chem.* **2013**, *36*, 6137-6146.
40
41
42
43 30. Sun, J.; Xu, H. *Molecules* **2010**, *15*, 8349-8359.
44
45
46
47 31. Long, G. C.; Harding, M. M.; Turner, T.; Hambley, T. W. *J. Chem. Soc., Dalton Trans.*
48 **1995**, 3905-3910.
49
50
51
52 32. Wo, J.; Kong, D.; Brock, N. L.; Xu, F.; Zhou, X.; Deng, Z.; Lin, S. *ACS Catal.* **2016**, *6*,
53 2831-2835.
54
55
56
57
58
59
60

- 1
2
3 33. Kottas, G. S.; Mehlstäubl, M.; Fröhlich, R.; De Cola, L. *Eur. J. Inorg. Chem.* **2007**, *22*,
4 3465-3468.
5
6
7
8
9 34. Xu, H.-B.; Deng, J.-G.; Zhang, L.-Y.; Chen, Z.-N.; *Cryst. Growth Des.* **2013**, *13*, 849-857.
10
11
12 35. Lv, B.; Wang, X.; Hu, H.-M.; Zhao, Y.-F.; Yang, M.-L.; Xue, G.; *Inorg. Chim. Acta.* **2016**,
13 453, 771-778.
14
15
16
17 36. Butler, C.; Goetz, S.; Fitchett, C.M.; Kruger, P.E.; Gunnalugsson, T.; *Inorg Chem.* **2011**,
18 50, 2723-2725.
19
20
21
22 37. Sakamoto, R.; Murata, M.; Kume, S.; Sampei, H.; Sugimoto, M.; Nishihara, H. *Chem.*
23 *Commun.* **2005**, 1215-1217.
24
25
26
27
28 38. Elmes, R. B. P.; Erby, M.; Bright, S. A.; Williams, D. C.; Gunnlaugsson, T. *Chem.*
29 *Commun.* **2012**, *48*, 2588-2590.
30
31
32
33 39. *Bruker APEX-3*, Bruker-AXS Inc., Madison, WI, 2016.
34
35
36
37 40. *SADABS*, Bruker-AXS Inc., Madison, WI, 2016.
38
39
40 41. Sheldrick, G. M. *Acta Crystallogr. Sect. A.* **2015**, *71*, 3-8.
41
42
43 42. Sheldrick, G. M. *Acta Crystallogr. Sect. C.* **2015**, *71*, 3-8.
44
45
46 43. Dolomanov, O. V.; Bourhis, L. J.; Gildea, R. J.; Howard, J. A. K.; Puschmann, H. *J. Appl.*
47 *Cryst.* **2009**, *42*, 339-341.
48
49
50 44. Zhang, X.-M. *Coord. Chem. Rev.* **2005**, *249*, 1201-1219.
51
52
53
54
55
56
57
58
59
60

- 1
2
3 45. Drew, M. G. B.; Harding, C. J.; McKee, V.; Morgan, G. G.; Nelson, J. *J. Chem. Soc.,*
4
5
6 *Chem. Commun.* **1995**, 1035-1038.
7
8
9 46. Desiraju, G. R.; Steiner, T. *The Weak Hydrogen Bond: In Structural Chemistry and*
10
11 *Biology*, Oxford University Press, Oxford, 2001.
12
13
14 47. Gu, Y.; Kar, T.; Scheiner, S. *J. Am. Chem. Soc.* **1999**, *121*, 9411-9422.
15
16
17 48. Desiraju, G. R. *Angew. Chem. Int. Ed.* **2011**, *50*, 52-59.
18
19
20 49. Burrows, A. D.; Cassar, K.; Friend, R. M. W.; Mahon, M. F.; Rigby, S. P.; Warren, J. E.
21
22 *CrystEngComm* **2005**, *7*, 548-550.
23
24
25 50. Quaresma, S.; André, V.; Martins, M.; Duarte, M. T. *J. Chem. Cryst.* **2015**, *45*, 178-188.
26
27
28 51. Spackman, M. A.; Jayatilaka, D. *CrystEngComm* **2009**, *11*, 19-32.
29
30
31 52. McKinnon, J. J.; Jayatilaka, D.; Spackman, M. A. *Chem. Commun.* **2007**, 3814-3816.
32
33
34 53. Furukawa, H.; Gándara, F.; Zhang, Y.-B.; Jiang, J.; Queen, W. L.; Hudson, M. R.; Yaghi,
35
36
37
38
39
40
41
42
43
44
45
46
47
48
49
50
51
52
53
54
55
56
57
58
59
60
- O. M. *J. Am. Chem. Soc.* **2014**, *136*, 4369-4381.
54. Burtch, N. C.; Jasuja, H.; Walton, K. S. *Chem. Rev.* **2014**, *114*, 10575-10612.
55. Hawes, C. S.; Hamilton, S. E.; Hicks, J.; Knowles, G. P.; Chaffee, A. L.; Turner, D. R.;
Batten, S. R. *Inorg. Chem.* **2016**, *55*, 6692-6702.
56. Chen, X.-M.; Tong, M.-L. *Acc. Chem. Res.* **2007**, *40*, 162-170.
57. Bauzá, A.; Mooibroek, T. J.; Frontera, A. *Chem. Commun.* **2015**, *51*, 1491-1493.
58. Bauzá, A.; Frontera, A.; Mooibroek, T. J. *Cryst. Growth Des.* **2016**, *16*, 5520-5524.

- 1
2
3 59. Frontera, A.; Gamez, P.; Mascal, M.; Mooibroek, T. J.; Reedijk, J. *Angew. Chem. Int. Ed.*
4
5 **2011**, *50*, 9564-9583.
6
7
8
9 60. Russell, V.; Scudder, M.; Dance, I. *J. Chem. Soc., Dalton Trans.* **2001**, 789-799.
10
11
12 61. Horn, C.; Scudder, M.; Dance, I. *CrystEngComm* **2000**, *2*, 53-66.
13
14
15 62. Moulton, B.; Zaworotko, M. J. *Chem. Rev.* **2001**, *101*, 1629-1658.
16
17
18 63. Makal, T. A.; Yakovenko, A. A.; Zhou, H.-C. *J. Phys. Chem. Lett.* **2011**, *2*, 1682-1689.
19
20
21
22
23
24
25
26
27
28
29
30
31
32
33
34
35
36
37
38
39
40
41
42
43
44
45
46
47
48
49
50
51
52
53
54
55
56
57
58
59
60

Table 1 Crystallographic and refinement parameters for all complexes

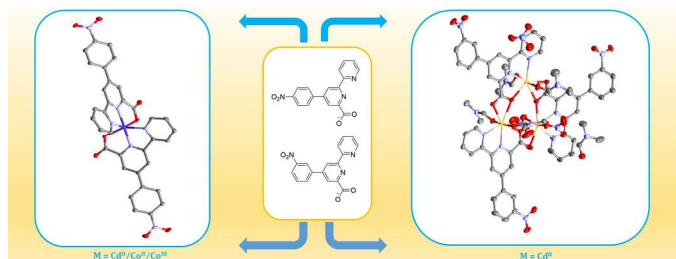
Identification code	1	2	3	4	5	6	8
Empirical formula	C ₃₄ H ₂₂ CdN ₆ O ₉	C ₃₄ H ₂₀ CdN ₆ O ₈	C ₆₃ H ₅₈ Cd ₃ N ₁₆ O ₂₆	C ₆₆ H ₆₅ Cd ₃ N ₁₇ O ₂₆	C ₃₄ H ₂₀ CoN ₆ O ₈	C ₃₄ H ₂₀ CoN ₇ O ₁₁	C ₃₄ H ₂₀ CoN ₇ O ₁₁
Formula weight	770.97	752.96	1792.45	1849.55	699.49	761.5	761.5
Temperature/K	100	100	100	100	100	100	100
Crystal system	triclinic	orthorhombic	triclinic	triclinic	monoclinic	triclinic	monoclinic
Space group	<i>P</i> -1	<i>Pna</i> 2 ₁	<i>P</i> -1	<i>P</i> -1	<i>C</i> 2/ <i>c</i>	<i>P</i> -1	<i>P</i> 2 ₁ / <i>n</i>
<i>a</i> /Å	10.6327(6)	30.908(3)	11.2959(5)	12.8513(6)	26.387(4)	8.054(3)	9.5657(13)
<i>b</i> /Å	10.8937(6)	7.4219(7)	19.0634(8)	16.0684(7)	8.4153(13)	13.418(4)	10.8843(15)
<i>c</i> /Å	13.7591(8)	25.239(2)	19.1406(8)	18.0214(9)	14.684(2)	15.092(5)	28.686(4)
α /°	87.4810(10)	90	112.735(2)	85.2710(10)	90	71.257(8)	90
β /°	89.2630(10)	90	105.212(2)	76.4100(10)	117.729(4)	76.306(8)	95.028(2)
γ /°	75.0120(10)	90	101.366(2)	86.4680(10)	90	83.362(9)	90
Volume/Å ³	1538.00(15)	5789.7(9)	3455.8(3)	3601.5(3)	2886.2(8)	1499.2(9)	2975.2(7)
<i>Z</i>	2	8	2	2	4	2	4
ρ_{calc} /g/cm ³	1.665	1.728	1.723	1.706	1.61	1.687	1.7
μ /mm ⁻¹	0.78	0.824	1.01	0.973	0.664	5.206	0.66
<i>F</i> (000)	776	3024	1800	1864	1428	776	1552
Crystal size/mm ³	0.3 × 0.19 × 0.18	0.09 × 0.06 × 0.05	0.19 × 0.02 × 0.01	0.16 × 0.07 × 0.03	0.45 × 0.19 × 0.02	0.07 × 0.07 × 0.04	0.14 × 0.06 × 0.04
Radiation	MoK α	MoK α	MoK α	MoK α	MoK α	CuK α	MoK α
2 θ range /°	2.962 to 55.16	4.842 to 52.03	2.458 to 50.996	3.264 to 52.982	3.488 to 51.998	6.962 to 136.452	2.85 to 51.998
Index ranges	-13 ≤ <i>h</i> ≤ 13, -14 ≤ <i>k</i> ≤ 12, -17 ≤ <i>l</i> ≤ 17	-38 ≤ <i>h</i> ≤ 38, -9 ≤ <i>k</i> ≤ 9, -31 ≤ <i>l</i> ≤ 31	-11 ≤ <i>h</i> ≤ 13, -21 ≤ <i>k</i> ≤ 23, -23 ≤ <i>l</i> ≤ 23	-16 ≤ <i>h</i> ≤ 16, -20 ≤ <i>k</i> ≤ 14, -22 ≤ <i>l</i> ≤ 22	-20 ≤ <i>h</i> ≤ 32, -10 ≤ <i>k</i> ≤ 10, -18 ≤ <i>l</i> ≤ 18	-9 ≤ <i>h</i> ≤ 9, -16 ≤ <i>k</i> ≤ 16, -18 ≤ <i>l</i> ≤ 17	-11 ≤ <i>h</i> ≤ 11, -13 ≤ <i>k</i> ≤ 13, -35 ≤ <i>l</i> ≤ 28
Reflns. collected	29313	89435	46478	53019	8799	15448	29069
Independent reflns.	7092 [R _{int} = 0.0379, R _{sigma} = 0.0377]	11368 [R _{int} = 0.1189, R _{sigma} = 0.0664]	12853 [R _{int} = 0.1573, R _{sigma} = 0.2269]	14709 [R _{int} = 0.0996, R _{sigma} = 0.1194]	2845 [R _{int} = 0.0921, R _{sigma} = 0.1259]	5452 [R _{int} = 0.0466, R _{sigma} = 0.0518]	5844 [R _{int} = 0.1146, R _{sigma} = 0.0987]
Reflns observed. [I ≥ 2 σ (I)]	5996	8985	5942	8327	1640	4799	3667
Data/restraints/parameters	7092/0/454	11368/19/884	12853/44/1037	14709/21/1019	2845/0/222	5452/0/478	5844/0/478
GooF on F ²	1.035	1.018	0.982	0.975	1.017	1.024	0.985
Final R indexes [I ≥ 2 σ (I)]	R ₁ = 0.0321, wR ₂ = 0.0691	R ₁ = 0.0456, wR ₂ = 0.0946	R ₁ = 0.0763, wR ₂ = 0.1281	R ₁ = 0.0517, wR ₂ = 0.1110	R ₁ = 0.0604, wR ₂ = 0.1060	R ₁ = 0.0406, wR ₂ = 0.1008	R ₁ = 0.0523, wR ₂ = 0.1000
Final R indexes [all data]	R ₁ = 0.0438, wR ₂ = 0.0737	R ₁ = 0.0699, wR ₂ = 0.1038	R ₁ = 0.2041, wR ₂ = 0.1622	R ₁ = 0.1251, wR ₂ = 0.1333	R ₁ = 0.1381, wR ₂ = 0.1296	R ₁ = 0.0462, wR ₂ = 0.1040	R ₁ = 0.1082, wR ₂ = 0.1165
Largest diff. peak/hole / e Å ⁻³	1.04/-1.09	1.72/-0.59	1.96/-1.72	1.83/-1.06	0.63/-0.93	0.31/-0.40	0.38/-0.42
Flack Parameter	N/A	-0.005(13)	N/A	N/A	N/A	N/A	N/A
CCDC Number	1544479	1544480	1544481	1544482	1544483	1544484	1544485

1
2
3
4
5
6
7
8
9
10
11
12
13
14
15
16
17
18
19
20
21
22
23
24
25
26
27
28
29
30
31
32
33
34
35
36
37
38
39
40
41
42
43
44
45
46
47
48
49
50
51
52
53
54
55
56
57
58
59
60

For Table of Contents Use Only

Crystal engineering of 6-carboxy-4-aryl-2,2'-bipyridine complexes: potent chelators with intrinsic intermolecular affinity

Hannah L. Dalton, Chris S. Hawes and Thorfinnur Gunnlaugsson



Two terdentate ligands based on the 6-carboxy-4-aryl-2,2'-bipyridine framework have been used in the synthesis of 8 new crystalline coordination compounds with Cd^{II}, Co^{II} and Co^{III} ions, consisting of mononuclear species or trinuclear cluster compounds. The electron deficient ligand backbone leads to significant polydentate C-H...O interactions which enforce strong crystal packing effects in the extended solid state structures of each complex